frontiers in Chemistry

ORIGINAL RESEARCH
published: 12 March 2021
doi: 10.3389/fchem.2021.650006

A Novel BODIPY Quaternary Ammonium Salt-Based Fluorescent Probe: Synthesis, Physical Properties, and Live-Cell Imaging

Peng Deng[1], *Fuyan Xiao*[2], *Zhou Wang*[3] *and Guofan Jin*[2]*

[1]The People's Hospital of Danyang, Affiliated Danyang Hospital of Nantong University, Zhenjiang, China, [2]School of Pharmacy, Jiangsu University, Zhenjiang, China, [3]College of Vanadium and Titanium, Panzhihua University, Panzhihua, China

The development of biological fluorescent probes is of great significance to the field of cancer bio-imaging. However, most current probes within the bulky hydrophobic group have limited application in aqueous medium and restricted imaging under physiological conditions. Herein, we proposed two efficient molecules to study their physical properties and imaging work, and the absorption and fluorescence intensity were collected with varying ions attending in aqueous medium. We enhance the water solubility through the quaternization reaction and form a balance between hydrophilic and hydrophobicity with dipyrrome-theneboron difluoride (BODIPY) fluorophore. We introduced pyridine and dimethylaminopyridine (DMAP) by quaternization and connected the BODIPY fluorophore by ethylenediamine. The final synthesized probes have achieved ideal affinity with HeLa cells (human cervical carcinoma cell line) in live-cell imaging which could be observed by Confocal Microscope. The probes also have a good affinity with subcutaneous tumor cells in mice in *in vivo* imaging, which may make them candidates as oncology imaging probes.

Keywords: BODIPY, quaternary ammonium salt, HeLa cells, *in vitro* imaging, *in vivo* imaging

OPEN ACCESS

Edited by:
Min Xue,
University of California, Riverside, United States

Reviewed by:
Zhonghan Li,
Oregon Health and Science University, United States
Hanjun Cheng,
Institute for Systems Biology (ISB), United States

***Correspondence:**
Guofan Jin
organicboron@ujs.edu.cn

Specialty section:
This article was submitted to Analytical Chemistry, a section of the journal Frontiers in Chemistry

Received: *06 January 2021*
Accepted: *01 February 2021*
Published: *12 March 2021*

Citation:
Deng P, Xiao F, Wang Z and Jin G (2021) A Novel BODIPY Quaternary Ammonium Salt-Based Fluorescent Probe: Synthesis, Physical Properties, and Live-Cell Imaging. Front. Chem. 9:650006. doi: 10.3389/fchem.2021.650006

INTRODUCTION

Small molecular probes with a high fluorescence signal are of use in cancer imaging development and play important roles in the study of biological activity and metabolism in cancer disease treatment (Gonzalez-Vera et al., 2020; Zhao et al., 2020; Zheng et al., 2020). There are many members in traditional fluorescent probes family, such as fluorescein, rhodamine, and some other potential probes (Chen et al., 2020; Ren et al., 2020; Zhong et al., 2020). With the continuous emergence of probes, small molecular fluorescent probes cut a striking figure in this field. One of these probes, named BODIPY, has become the key subject in the view of researchers, due to its excellent photophysical properties and the advantage of easy modification (Liu et al., 2020; Wang H. et al., 2020). However, there are still many problems to be solved for the structural modification of BODIPY, such as its highly structural complexity and poor water solubility. Based on this, a simple and convenient preparation method from easily available raw materials also needs to be proposed.

Aqueous systems are essential in life processes and the global environment. But traditional BODIPY dyes are only soluble in organic solvents, and their low solubility mean they have limited application in biological fields. To this end, H.J. Worries introduced a chlorosulfonic acid group to

the core structure in 1985, which markeda key first step to advancing water solubility (Choi et al. 2018). Inspired by this, some related work on improving solubility has been carried out. The water solubility of BOPIDY can be improved by introducing different types of hydrophilic groups such as sulfonate (Koh et al., 2019), phosphonate, and quaternary ammonium salt (Mao et al., 2020; Zhou et al., 2020). Common water-soluble modification occurs in the core structure or boron atom center, and the 2, 6 or 3, 5 sites are common modification sites. Even though many works are studying the exploration of hydrophilicity, it remains superficial, which has caused certain obstacles to the imaging application of compounds. Research on the development of fluorescent probes with a simplified structure and enhanced water solubility is still in its infancy stage and more work needs to be done in the future.

As a noticeable probe synthesized since 1968, BODIPY has many new biological applications which have been gradually discovered and gained more and more attention (Wang R. et al., 2020; Xu et al., 2020). Live cell imaging is a great example of these applications (Guasch-Ferre et al., 2020; Wang F. et al., 2020). It is an important practice in biomedical study for the analysis of the functional and pathological of cells and tissues and clinical diagnosis. Water soluble modification opens up a new avenue for bioactivity research, including cell imaging and research on water-soluble probes for imaging, the study of which has gradually increased (Callmann et al., 2020; Liang et al., 2020). For example, Jin et al. synthesized a new water-soluble compound (4,4-di-(4′-methylmercaptophenoxy)-8-(N-methylpyridinium-2-yl)-1,3,5,7-tetramethyl-4-bora-3a,4a-diaza-s-indacene) and successfully applied it to imaging in living cells (Wegner and Zimmermann, 2004; Khailova et al., 2020; Tang et al. 2020).

In this paper, we report two novel water-soluble fluorescent probes, BDP-1 and BDP-2, for live cell imaging. The unique BODIPY core with strong fluorescence properties provides new possibilities for cell imaging and metabolism research. In the probe design work, the balance between hydrophilicity and lipophilicity is comprehensively considered. The hydrophobicity fluorescein pyrrole nucleus acts as the fluorophore. The side chain ethylenediamine bridge group is introduced to adjust its water-lipid balance. Finally, the N-choloropyridinium with a positive charge moiety group acts as a water-soluble improving part. In this paper, the concise synthetic strategy of novel BODIPY probes has been proposed and the optical properties in the presence of different ions are also explored. The probes have achieved ideal non-specific affinity with HeLa cells (human cervical carcinoma cell line) in live cell imaging and a good non-specific affinity with subcutaneous tumor cells in mice in *in vivo* imaging.

MATERIALS AND METHODS

General Materials

The acetonitrile solvent used in the reaction was distilled by calcium hydride in advance. In the characterization part, the ^{1}H and ^{13}C spectra were recorded on Bruker Avance spectrometer (400 MHz for ^{1}H, 101 MHz for ^{13}C) in CD_3OD with the Me_4Si at chemical shifts δ 0.00 ppm as standard to characterize the structures. Ultraviolet-visible (UV-vis) and fluorescence spectra were recorded on a UV-2550 spectrophotometer and Shimadzu RF-5301PCS spectrofluorophotometer, respectively, at room temperature.

Synthesis

Synthesis of 7-chloro-2-ethyl-5,5-difluoro-1,3-dimethyl-10-phenyl-5H-4l4,5l4-dipyrrolo[1,2-c:2′,1′-f] [1,3,2]diazaborinine (1).

The compound 1 was synthesized from 2-chloro-5-benzoyl-pyrrole (0.8 g, 4.0 mmol), $POCl_3$ (2 ml), and 2,4-dimethyl-3-ethylpyrrole (1.8 g, 15.0 mmol) in dichloromethane through stirring for 24 h at room temperature. Neutralization by $NaHCO_3$ was carried out to obtain the intermediate. Et_3N (2 ml) was added into the intermediate in toluene and BF_3·OEt (2 ml) was added by stirring for 7 h at 100°C. Neutralization by $NaHCO_3$ was carried out again and purification by column chromatography to gain 1 was used (0.5 g, 41%).

Synthesis of (Z)-N1-(1-(difluoroboranyl)-5-((4-ethyl-3,5-dimethyl-2H-pyrrol-2-ylidene) (phenyl)methyl)-1H-pyrrol-2-yl)ethane-1,2-diamine (2).

(Z)-2-chloro-1-(difluoroboranyl)-5-((4-ethyl-3,5-dimethyl-2H-pyrrol-2-ylidene) (phenyl)methyl)-1H-pyrrole (0.3 g, 0.8 mmol) was mixed with the dry acetonitrile solution of ethane-1,2-diamine (0.1 g, 1.7 mmol) with the attendance of triethylamine (0.2 g, 1.3 mmol) and stirred for 6 h at room temperature. The reaction mixture was evaporated and purified by silica gel column chromatography to obtain 2 in red powder (0.3 g, 91%). ^{1}H NMR (400 MHz, $CDCl_3$) δ 7.42–7.40 (m, 3H), 7.31–7.29 (m, 2H), 6.46 (d, J = 4.4 Hz, 1H), 5.92 (d, J = 4.8 Hz, 1H), 3.409 (s, 2H), 3.00 (t, J = 6.0 Hz, 2H), 2.47 (s, 3H), 2.35–2.29 (dd, J = 7.6, 14.8 Hz, 2H), 1.37 (s, 3H), 0.99 (t, J = 7.6 Hz, 3H). ^{13}C NMR (100 MHz, $CDCl_3$) δ 159.8, 144.9, 135.2, 133.3, 133.1, 132.4, 132.3, 130.0, 129.6, 128.3, 128.0, 106.0, 46.8, 41.4, 29.7, 17.1, 15.0, 11.9, 11.6. ITMS (ESI) calculated for $C_{21}H_{25}BF_2N_4$ $[M + H]^+$ m/z 383.2218; found 383.2345.

General synthesis procedure of 1-(2-((2-((8-ethyl-5,5-difluoro-7,9-dimethyl-10-phenyl-5H-5l4,6l4-dipyrrolo[1,2-c:2′,1′-f] [1,3,2]diazaborinin-3-yl)amino)ethyl)amino)-2-oxoethyl)pyridin-1-ium chloride (BOD-1) and 4-(dimethylamino)-1-(2-((2-((8-ethyl-5,5-difluoro-7,9-dimethyl-10-phenyl-5H-5l4,6l4-dipyrrolo[1,2-c:2′,1′-f][1,3,2]diazaborinin-3-yl)amino)ethyl)amino)-2-oxoethyl) pyridin-1-ium chloride (BOD-2).

Oxalyl chloride (0.2 ml, 3.0 mmol) was slowly dropwised to the previously synthesized 2 (0.3 g, 1.0 mmol) under ice bath temperature with 5 ml acetonitrile as a solvent. The reaction was over after 10 min and purified by silica gel column chromatography to obtain 3. The pyridine (3 ml, 37 mmol) or DMAP (0.08 g, 0.7 mmol) was mixed with 3 (0.05 g, 0.1 mmol) in a pressure tube and the resulted mixture was heated at 50°C for 8 h. From that, DMAP was reacted in 2 ml acetonitrile, while pyridine acted as a solvent. Then the reaction was evaporated by rotary evaporation and washed with 3 ml EtOAc and Petroleum ether (1: 3) to obtain pure crimson solid.

SCHEME 1 | Chemical structure design and mechanism.

Synthesis Procedure of BOD-1

The pyridine (3 ml, 37 mmol) was mixed with 3 (0.05 g, 0.1 mmol) according to the general procedure to obtain pure powder BDP-1 (0.04 g, 68.2%). ^{1}H NMR (400 MHz, CD_3OD) δ 8.62 (d, J = 4.4 Hz, 2H), 8.10 (t, J = 6.8 Hz, 1H), 7.49 (t, J = 2 Hz, 3H), 7.31–7.29 (m, 2H), 6.50 (d, J = 4.8 Hz, 1H), 6.20 (d, J = 4.8 Hz, 1H), 5.47 (s, 2H), 3.56 (s, 4H), 3.34 (m, 2H), 3.07 (d, J = 10 Hz, 1H), 2.44 (s, 3H), 2.37 (d, J = 7.6 Hz, 2H), 1.39 (s, 3H), 1.03 (t, J = 7.6 Hz, 3H). ^{13}C NMR (100 MHz, CD_3OD) δ 165.1, 160.3, 148.3, 146.1, 146.0, 143.5, 135.2, 133.1, 132.8, 132.4, 131.1, 129.5, 128.8, 127.9, 127.5, 121.4, 106.8, 61.6, 43.0, 39.3, 16.6, 14.1, 10.7, 10.4. HR-MS (FAB) calculated for $C_{28}H_{31}BClF_2N_5O$ [(M-BF2)$^+$-Cl$^-$] m/z, 454.26014, observed 454.25972.

Synthesis Procedure of BDP-2

This was carried out according to the general procedure to obtain pure crimson powder BDP-2 (0.03 g, 47.4%). ^{1}H NMR (400 MHz, $CDCl_3$) δ 8.13 (d, J = 6.2 Hz, 2H), 8.01 (s, 1H), 7.48 (d, J = 4.7 Hz, 3H), 7.41 (d, J = 3.5 Hz, 2H), 7.29 (d, J =4.3 Hz, 2H), 6.99 (d, J = 6.5 Hz, 2H), 6.88 (d, J = 5.6 Hz, 2H), 6.53–6.44 (m, 1H), 6.23 (s, 1H), 3.54 (d, J = 14.2 Hz, 4H), 3.25 (s, 6H), 2.43 (d, J = 5.6 Hz, 3H), 2.38 (dd, J = 7.6 Hz, 2H), 1.38 (d, J = 4.8 Hz, 3H), 1.00 (t, J = 7.6 Hz, 3H). ^{13}C NMR (100 MHz, CD_3OD) δ 166.9, 157.7, 156.6, 147.8, 142.9, 138.7, 135.2, 134.3, 133.1, 132.5, 130.8, 129.5, 128.3, 127.9, 122.3, 107.1, 106.8, 58.1, 43.0, 38.9, 38.8, 16.6, 14.1, 10.7, 10.4. HR-MS (FAB) calculated for $C_{30}H_{36}BClF_2N_6O$ [(M-BF2)$^+$-Cl$^-$] m/z, 497.30234, observed 497.30167.

Photophysical Properties and Sensing of Target Ions

Ultraviolet-visible (UV-vis) and fluorescence spectra were recorded on a UV-2550 spectrophotometer and Shimadzu RF-5301PCS spectrofluorophotometer, respectively, at room temperature. The mother liquor for sensing in aqueous solution was prepared at concentration of 5 mM and diluted into the desired concentration. The spectra data was collected by the above instruments under different preset concentrations with the absence and attendance of eight target ions after mixing evenly.

Transmission Electron Microscope Analysis

Transmission electron microscopy of compounds (10 μM) BDP-1 and BDP-2 was conducted in methanol. The sample of the configured electron microscope was dissolved in methanol solution, and the pictures were collected by transmission electron microscope (Japan Electronics, JEM-1400plus) at room temperature.

Cytotoxicity Analysis

HCT-116, Hela, and normal liver L-02 cells were screened for *in vitro* cytotoxicity, and all were purchased from the American type culture collection (United States). HCT-116 and Hela cells were routinely cultured in RPMI-1640, while L-02 cells were routinely cultured in DMEM. 10% fetal bovine serum (FBS, purchased from Hangzhou Sijiqing Biological Engineering Materials Co., Ltd.) was added to the medium, and the cells were sub-melted in a humidified atmosphere at 37°C and 5% CO_2. These cells were monitored daily and maintained at 80% cell density.

MTT cancer cells (HCT-116 and Hela) and normal human lung L-02 were tested for the cytotoxicity of each cell line in the logarithmic growth phase. All cells were seeded on 96-well plates at a rate of 106 cells per well. Then they were treated with berberine or compounds (BDP-1, BDP-2) at different concentrations, and the samples were tested for 24 h. Supernatant was dissolved in 100 ml DMSO and shaken for 10 min. The optical density of the sample was measured at 490 nm with a microplate photometer. Cell viability was expressed as the percentage change in absorbance relative to the control value.

Hela Cervical Cancer Live Cell Imaging

Hela Cells were incubated with different BODIPY derivatives, BDP-1 and BDP-2 (5 mM, 2 μL), for 1 h at 37°C after good cultivation and washing. The culture medium was separated and discarded and treated with PBS afterward; the stained cells were then observed under the confocal laser scanning microscope with the emission wavelengths between 500–510 nm. Hela cells were also stained with DAPI (5 μg/ml) under the same operating procedures as the control group and images were collected.

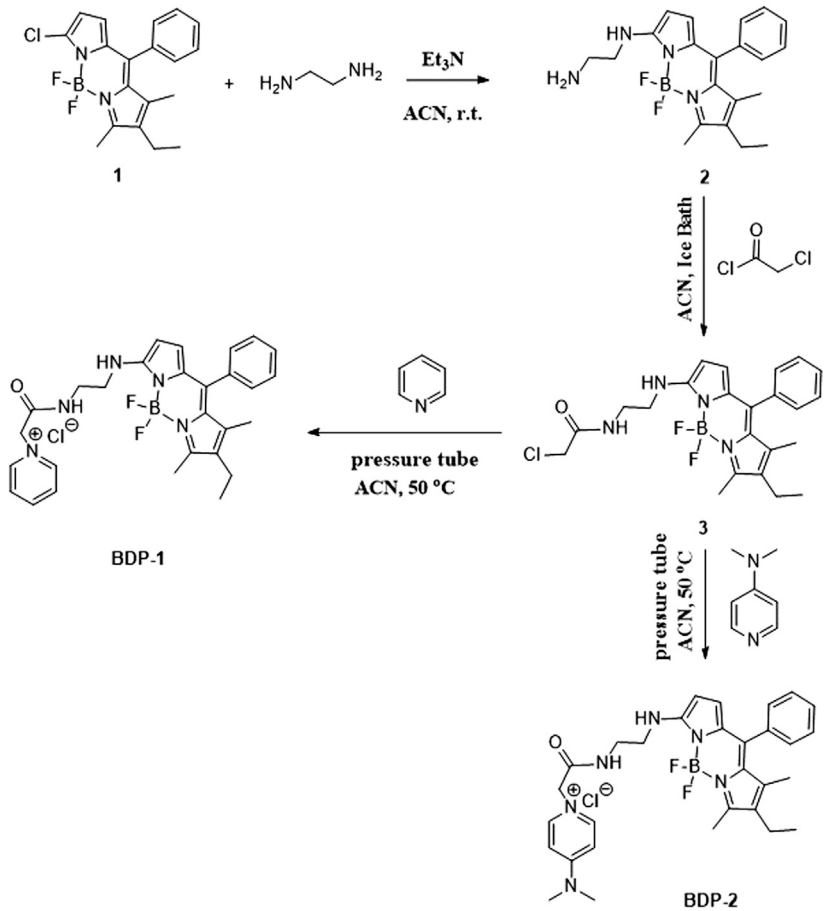

SCHEME 2 | Synthetic route to the water-soluble N-choloropyridinium BODIPYs.

In vivo Experiment

Animal studies were conducted under institutional approval (Laboratory Animal Center of Jiangsu University, Zhenjiang, China). Two mouse components weighing 21 g and 20 g were used for *in vivo* imaging experiments. BDP-1 (20 μM) and BDP-2 (20 μM) were added by intraperitoneal injection under fasting conditions and fluorescence was collected after 30 min of exposure.

RESULT AND DISCUSSION

Chemistry

For the design, the fluorescent excimer is the (Z)-1-(difluoroboranyl)-2-((4-ethyl-3,5-dimethyl-2H-pyrrol-2-ylidene) (phenyl)methyl)-1H-pyrrole, and the BF_2 unit inside this group can generate the intense emission band from S_1 to S_0 transition through the flow of electrons inside the molecule. As shown in Scheme 1, the green carbonyl amine part in the middle acts as a water-solubility part which is a vital bridge between the fluorescence core and the hydrophilic functional part. The hydrophilic pyridine moiety plays an important role in improving the biocompatibility and water solubility of the compound and it produces a marked effect by forming a super-hydrophilic quaternization structure. In addition, the positive charge enriches the target anion response in aqueous medium. Meanwhile, the oxygen-enriched and nitrogen-rich part in the structure as acts as a hydrogen bond donor or acceptor, which is beneficial to the improvement of live cell imaging. In summary, the powerful combination of the three parts provides unprecedented new ideas for the structural modification of BODIPY, and also adds color to the application of fluorescent probes for cancer cell imaging.

As shown in Scheme 2, the probes were synthesized in a few short steps. The compound 1 was synthesized from 2-chloro-5-benzoyl-pyrrole and 2,4-dimethyl-3-ethylpyrrole with the attendance of $POCl_3$ in dichloromethane, with triethylamine and boron trifluoride etherate subsequently added (Suzuki et al., 2006; Carrascal et al., 2019; Li et al., 2019). We synthesized BDP-1 and BDP-2 starting from compound 1 followed by nucleophilic substitution with ethylenediamine and subsequently by acyl chlorination with chloroacetyl chloride to obtain intermediate 3. The intermediate 3 was quaternized with pyridine and 4-dimethylaminopyridine to improve the biocompatibility and increase the water solubility of the products.

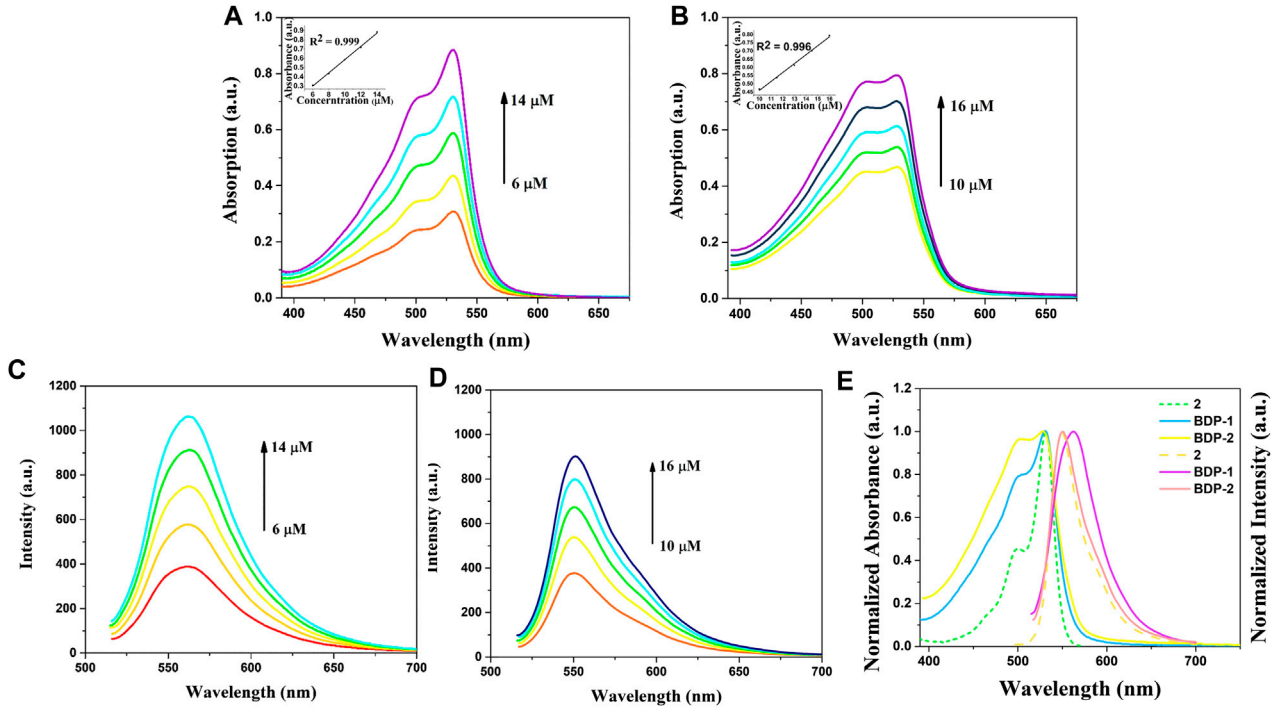

FIGURE 1 | Absorption and emission spectra of BDP-1 and BDP-2. Absorption spectra of **(A)** BDP-1 and **(B)** BDP-2 in methanol at 25°C. Emission spectra of **(C)** BDP-1 and **(D)** BDP-2 in methanol at 25°C. (concentration BDP-1: 6, 8, 10, 12, 14 μM; BDP-2: 10, 11.5, 13, 14.5, 16 μM). **(E)** Normalized spectrum of 2, BDP-1 and BDP-2. Insert: The absorption changes upon the increasing concentration.

TABLE 1 | Absorption and emission data.[a]

Compound	$\lambda_{max,abs}$ (nm) ($\varepsilon/10^5$ L·mol^{-1}·cm^{-1})	$\lambda_{max,emi}$ (nm)
2	530 (0.300)	550
BDP-1	530 (0.717)	560
BDP-2	528 (0.544)	550

[a]*Measurements were performed in MeOH unless otherwise noted. The excitation wavelength is 500 nm for 2, BDP-1, and BDP-2.*

TABLE 2 | Cytotoxicity analysis of BDP-1 and BDP-2 with the drug berberine as reference.

Comp.	IC_{50} (μM) ± SD		
	HCT-116	Hela	L-02
BDP-1	125.62 ± 3.70	110.46 ± 8.43	28.69 ± 8.73
BDP-2	103.83 ± 2.98	97.28 ± 11.93	33.78 ± 5.16
Berberine	29.47 ± 9.19	21.26 ± 3.11	>150

Photophysical Properties

The optical spectra were also characterized in methanol at room temperature for its photophysical properties in **Figure 1** and **Table 1**. The absorption spectrum data of BDP-1 and BDP-2 were collected in the concentration range from 6 to 14 μM and 10 to 16 μM, respectively, to keep it at an applicable range according to Lambert Beer's law. As shown in **Figure 1**, the absorption band of BDP-1 was similar in shape and peaks to BDP-2, retaining the maximum absorptions at 530 and 528 nm, respectively. The fluorescence spectra of BDP-1 showed maximum at 560 nm, although it showed a slightly greater red shift than that of BDP-2 and 2 (λ_{em} = 550 nm). This phenomenon may indicate that the fluorophore is served by the BODIPY core, and the introduced pyridine group does not negatively affect the fluorescence effect of the compound while providing an indicator of its hydrophilicity. Therefore, intensive fluorescence and proper hydrophilic-lipophilic equilibrium can serve as candidates for excellent cell imaging.

Absorption and emission studies for ion response experiments were carried out and the result was shown in **Figure 2**. The results show that the compounds spectra did not change after the addition of of many ions (Cl^-, F^-, Br^-, I^-, Ca^{2+}, and Zn^{2+}), while the absorption peaks of HS^- ions are conspicuously blue-shifted from 500 to 450 nm accompanied by a significant decline in absorption spectra. Analysis of absorption spectroscopy results showed that BDP-1 has a more obvious effect on HS^- than other ions and produces a more obvious decrease in absorbance than BDP-2. The fluorescence emission spectrum recording situation is similar to the absorption spectrum which responds to H_2S distinctly. Surprisingly, in the presence H_2S, the fluorescence appears to increase slightly and differ from the addition of other tested ions. In the end, we deduce the reason for the fluorescence enhancement may be that the ionization of the active ions in water hinders the electron flow between the pyridine group and the fluorophore in the structure, and then affects the

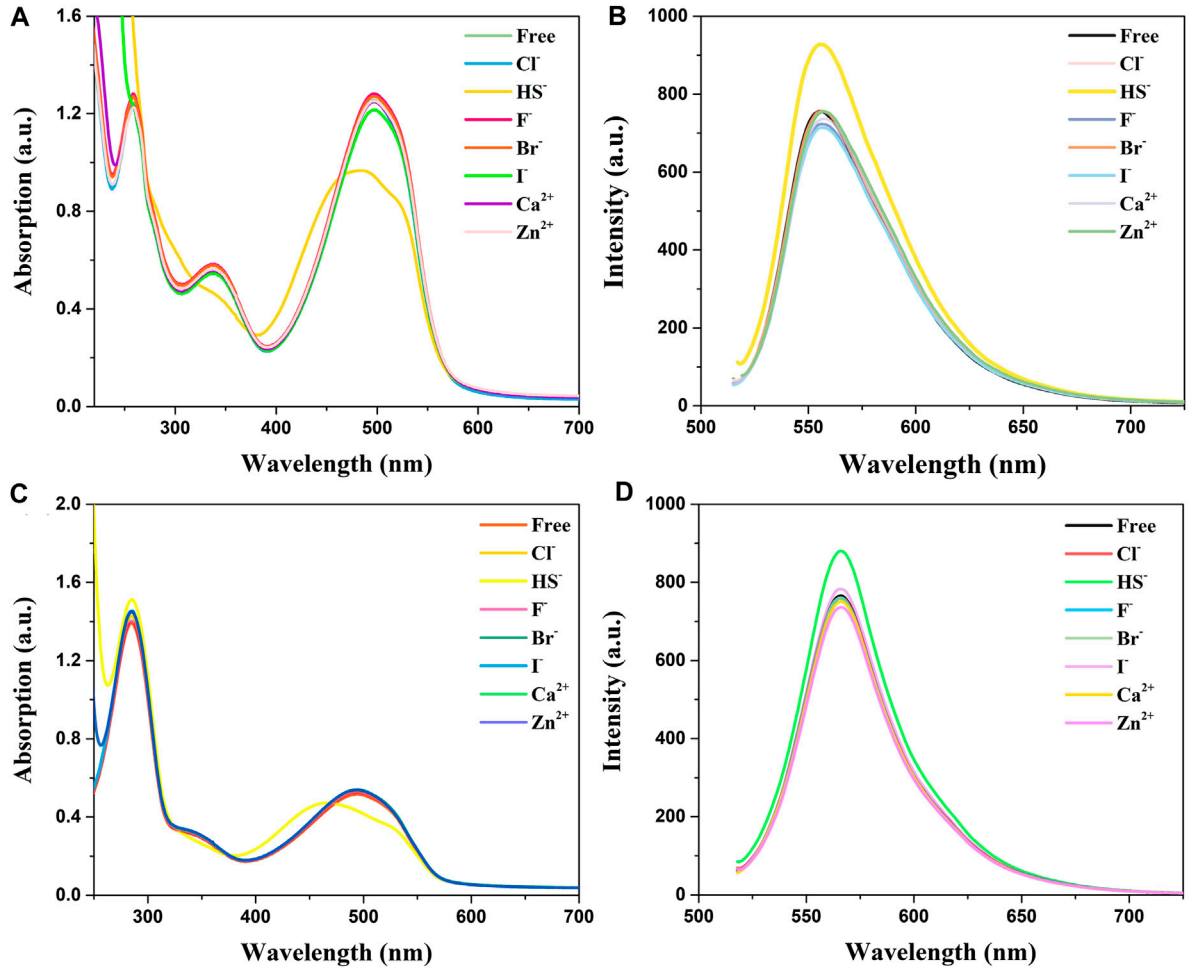

FIGURE 2 | Absorption and fluorescence responses of probes to ions (100 μM) in aqueous solution. **(A)** Absorption and **(B)** Fluorescence spectra of BDP-1 (10 μM); **(C)** Absorption and **(D)** Fluorescence spectra of BDP-2 (10 μM). (1) Free; (2) Cl^{-}; (3) NaHS; (4) F^{-}; (5) Br^{-}; (6) I^{-}; (7) Ca^{2+}; (8) Zn^{2+}. Data were recorded 10 min after the addition of different ions.

intramolecular electron transfer. And in order to prove this hypothesis, the following experiment was conducted.

In addition, the optical response of BDP-1 and BDP-2 to HS^{-} obviously depended on the volume fraction of water (fw) in the water/MeOH mixture which responded under all circumstances. As shown in **Figure 3** (solid line), the methanol-dissolved BDP-1 maintained a sharper peak at 528 nm than that of the full water solvent with a blunt peak at 500 nm. It could be seen that, as the fw value gradually grows from 50 to 100%, the property of probes changed a lot in peak shape and maximum absorbance. On the other hand, after adding HS^{-} (short dot line), the spectrum changes obviously in morphology and peaks. The methanol dissolved BDP-1 still maintained a small peak at 528 nm with an evident blueshift from 528 nm to 450 nm with an increase of fw value. In detail, for the HS^{-}-activated absorption transition, both the morphology and the distribution of absorption peaks showed a gradual reduction to lower and this phenomenon can be clearly reflected in pure water (fw = 100%). Furthermore, BDP-2 has a similar situation, with the strongest response changes in pure water. Therefore, in the presence of different volume fractions of water (fw), it has a stable response activity to H_2S as expected, so it has great potential for application research. This phenomenon could also prove our previous hypothesis that ionization in aqueous solution induces fluorescence enhancement.

In addition, to further observe the morphology of the quaternized compounds, the structure characterization was also carried out by transmission electron microscope (TEM) characterization in methanol at 25°C, and the self-assembly BDP-1 and BDP-2 structures were clearly presented. As can be seen in the image (**Supplementary Figure S10**), the compound is in a state of aggregation in the solution. This aggregation may be inferred to be caused by the positive charge of the compound itself resulting in it layering itself on top of each other; thus, the aggregation becomes like the picture.

It is interesting to analyze anti-proliferation as shown in **Figure 4**. IC_{50} values of 125.62 ± 3.70 and 103.83 ± 2.98 μM were observed for BDP-1 and BDP-2 in HCT-116 cells at 37°C,

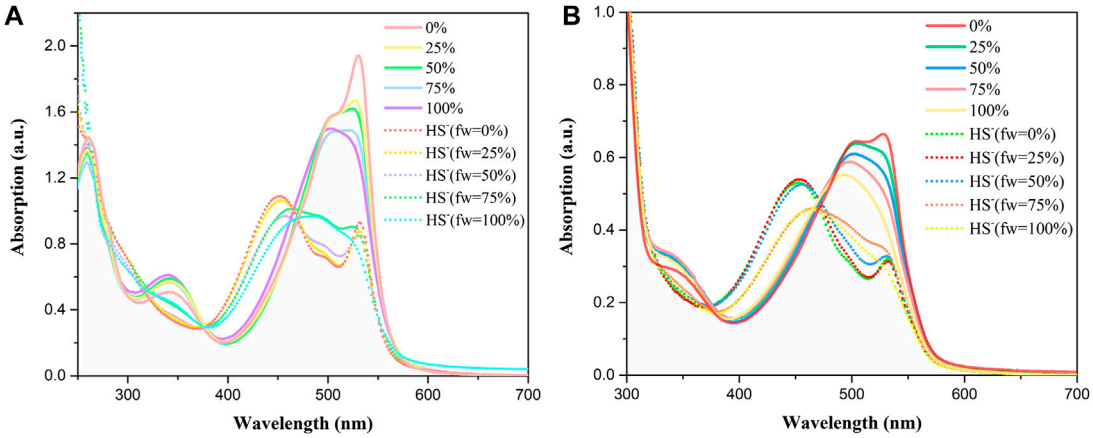

FIGURE 3 | Absorption spectra at different fw (water/methanol) of **(A)** BDP-1 (10 μM) and **(B)** BDP-2 (10 μM) at 25°C (solid line), with the addition of NaHS at 25°C (short dot line).

respectively IC_{50} values of 110.46 ± 8.43for 5 and 97.28 ± 11.93 μM for 6 in HeLa cell line were observed. For a non-cancerous lung cell line (L-02), the toxicity of 5 (28.69 ± 8.73 μM) and 6 (33.78 ± 5.16 μM) is not ideal compared to the reference drug and should be improved in further study. Therefore, reducing the toxicity to normal cells and adjusting the balance between the water-solubility and bioactivity is also a required direction.

The BDP-1 and BDP-2 presents obvious aggregation and displayed good stability in methanol solvent under the 200 nm scale. Meanwhile, the presence of positive charges in the structure leads to the stacking of layers. It could also infer that it keeps the balance between the hydrophilicity and lipophilicity of the compounds to achieve amphiphilicity, which may lead to this polymerization.

Moreover, the fluorescence performance in cell imaging means a lot for the application of probes in the fluorescent family. HeLa cells were incubated with BODIPYs for 30 min for cell imaging study. Then the imaging results were shown in **Figure 5**, and it could be directly observed that both BDP-1 and BDP-2 were uptaken by the HeLa cell membrane with desired fluorescence imaging. Both BODIPY derivatives show higher fluorescence than the non-quaternized compound 2. It could be deduced that the compounds were absorbed into the cell membrane and then firmly targeted to the cells due to the positive charge and the counterpoise of hydrophilic and lipophilic. Then they emit strong fluorescence in intracellular structures.

In vivo fluorescence experiments in mice were designed and executed. BDP 1 and BDP 2 (10 mM) were intraperitoneally injected under fasting conditions in mice. After 40 min of exposure, the fluorescence intensity of the tumor tissue was detected. As shown in **Figure 6**, *in vivo* fluorescence is generated in subcutaneous tumors. It is reasonable that the fluorescence intensity of the two compounds is high and the fluorescence brightness is sensitive. Finally, it can be observed that the precise generation and penetration of fluorescence in subcutaneous tumors have the potential for further medical imaging applications.

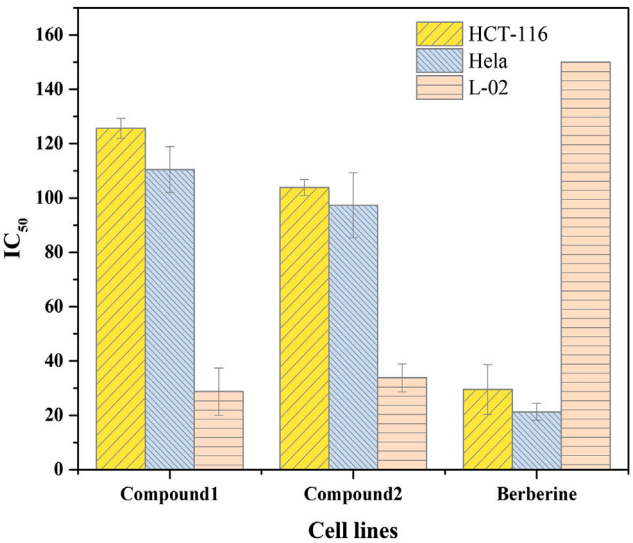

FIGURE 4 | Cytotoxicity analysis of BDP-1 and BDP-2 with the drug berberine as reference.

CONCLUSION

In conclusion, we designed and prepared two water-soluble small molecule probes that have ideal fluorescence intensity and good potential for cancer cell imaging applications. Traditional small-molecule fluorophores have the shortcomings of low water solubility and weak fluorescence, however, the BODIPYs synthesized in this paper could not only generate high intensity fluorescent, but also solve the problem of water solubility. What's more, they could also serve as potential

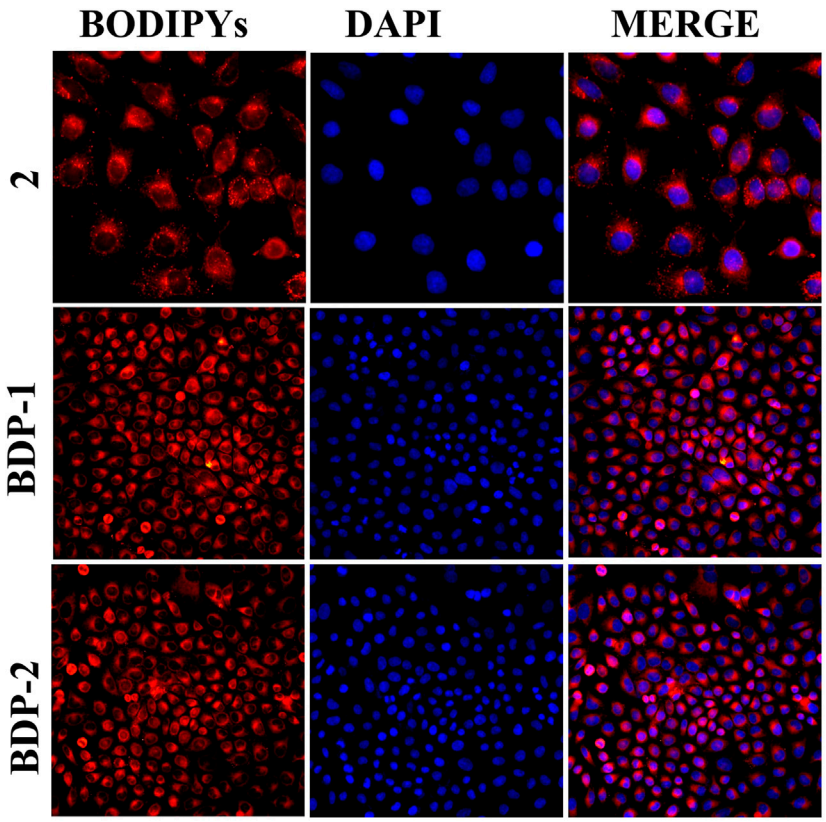

FIGURE 5 | Cell imaging stained with samples under different compounds: compound 2, BDP-1, and BDP-2 treatment.

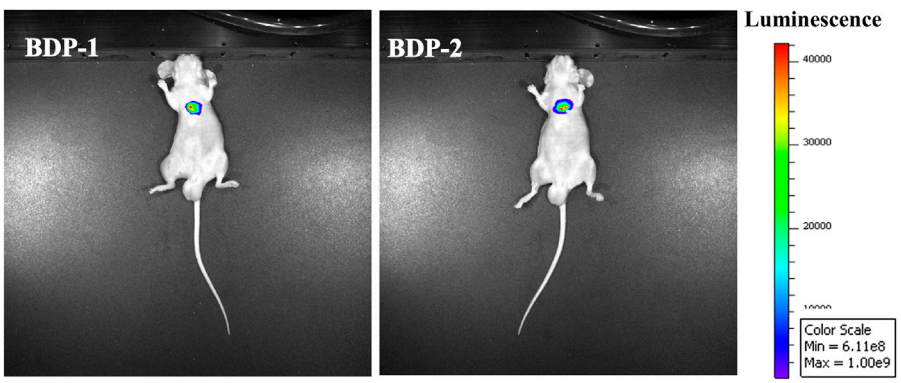

FIGURE 6 | *In vivo* fluorescence images of mice after injection of BDP-1 (10 mM) and BDP-2 (10 mM).

probes in aqueous solution. The application of cell imaging contributes to intracellular visualization for biological study. The newly synthesized probes with excellent photophysical properties have a broad development prospect, which lay a foundation for further research on water-soluble ion probes.

DATA AVAILABILITY STATEMENT

The original contributions presented in the study are included in the article/**Supplementary Material**, further inquiries can be directed to the corresponding author.

AUTHOR CONTRIBUTIONS

PD mainly responsible for *in vivo* imaging experiments; FX and ZW were responsible for the collation and characterization of experimental data. GJ responsible for writing and reviewing papers.

FUNDING

This study was supported financially by the scientific research foundation of Jiangsu University (Grant No. 5501290005).

ACKNOWLEDGMENTS

The authors would like to express their thanks for the biological experimental data provided by the people's Danyang hospital Jiangsu University.

SUPPLEMENTARY MATERIAL

The Supplementary Material for this article can be found online at: https://www.frontiersin.org/articles/10.3389/fchem.2021.650006/full#supplementary-material.

REFERENCES

Callmann, C. E., Cole, L. E., Kusmierz, C. D., Huang, Z., Horiuchi, D., and Mirkin, C. A. (2020). Tumor cell lysate-loaded immunostimulatory spherical nucleic acids as therapeutics for triple-negative breast cancer. *Proc. Natl. Acad. Sci. U.S.A.* 117, 17543–17550. doi:10.1073/pnas.2005794117

Carrascal, J. J., Villegas, J. M., Baena-Aristizabal, C. M., Baena, Y., and Perez, L. D. (2019). Nanoparticles based on a PEGylated methacrylate copolymer as vehicles for hydrophilic antimicrobial additives: a study on chemical interactions with a benzoic acid probe molecule. *Colloid Polym. Sci.* 297, 809–820. doi:10.1007/s00396-019-04502-9

Chen, Z., Xu, X., Meng, D., Jiang, H., Zhou, Y., Feng, S., et al. (2020). Dual-emitting N/S-doped carbon dots-based ratiometric fluorescent and light scattering sensor for high precision detection of Fe(III) ions. *J. Fluoresc.* 30, 1007–1013. doi:10.1007/s10895-020-02571-6

Choi, E. K., Park, S. H., Lim, J. A., Hong, S. W., Kwak, K. H., Park, S. S., et al. (2018). Beneficial role of hydrogen sulfide in renal ischemia reperfusion injury in rats. *Yonsei Med. J.* 59, 960–967. doi:10.3349/ymj.2018.59.8.960

Gonzalez-Vera, J. A., Lv, F., Escudero, D., Orte, A., Guo, X., Hao, E., et al. (2020). Unusual spectroscopic and photophysical properties of solvatochromic BODIPY analogues of Prodan. *Dyes Pigm.* 182, 108510. doi:10.1016/j.dyepig.2020.108510

Guasch-Ferre, M., Santos, J. L., Martínez-González, M. A., Clish, C. B., Razquin, C., Wang, D., et al. (2020). Glycolysis/gluconeogenesis-and tricarboxylic acid cycle-related metabolites, Mediterranean diet, and type 2 diabetes. *Am. J. Clin. Nutr.* 111, 835–844. doi:10.1093/ajcn/nqaa016

Khailova, L. S., Vygodina, T. V., Lomakina, G. Y., Kotova, E. A., and Antonenko, Y. N. (2020). Bicarbonate suppresses mitochondrial membrane depolarization induced by conventional uncouplers. *Biochem. Biophys. Res. Commun.* 530, 29–34. doi:10.1016/j.bbrc.2020.06.131

Koh, X. Y., Koh, X. H., Hwang, L., Ferrer, F. J., Rahmat, S. A. B., Lama, D., et al. (2019). Therapeutic anti-cancer activity of antibodies targeting sulfhydryl bond constrained epitopes on unglycosylated RON receptor tyrosine kinase. *Oncogene* 38, 7342–7356. doi:10.1038/s41388-019-0946-8

Li, Y., Wu, H., Sun, N., and Deng, C. (2019). Fabrication of hydrophilic multilayer magnetic probe for salivary glycopeptidome analysis. *J. Chromatogr. A.* 1587, 24–33. doi:10.1016/j.chroma.2018.11.040

Liang, Y. C., Gou, S. S., Liu, K. K., Wu, W. J., Guo, C. Z., Lu, S. Y., et al. (2020). Ultralong and efficient phosphorescence from silica confined carbon nanodots in aqueous solution. *Nano Today* 34, 100900. doi:10.1016/j.nantod.2020.100900

Liu, H., Xu, G., Zhu, T., Wang, R., Tan, J., Zhao, C., et al. (2020). Rational design of water-dispersible and biocompatible nanoprobes with H_2S-triggered NIR emission for cancer cell imaging. *J. Mater. Chem. B* 8, 6013–6016. doi:10.1039/d0tb00173b

Mao, Z., Yang, X., Mizutani, S., Huang, Y., Zhang, Z., Shinmori, H., et al. (2020). Hydrogen sulfide mediates tumor cell resistance to thioredoxin inhibitor. *Front. Oncol.* 10, 252. doi:10.3389/fonc.2020.00252

Ren, H., Wu, P., Li, F., Yu, S., Jin, L., and Lou, D. (2020). Development of a colorimetric and fluorescent Cu^{2+} ion probe based on 2′- hydroxy-2,4-diaminoazobenzene and its application in real water sample and living cells. *Inorg. Chim. Acta* 507, 119583. doi:10.1016/j.ica.2020.119583

Suzuki, I., Ui, M., and Yamauchi, A. (2006). Supramolecular probe for bicarbonate exhibiting anomalous pyrene fluorescence in aqueous media. *J. Am. Chem. Soc.* 128, 4498–4499. doi:10.1021/ja055772f

Tang, M., Zhao, X., Hu, Y., Zeng, M., and Song, C.-P. (2020). Arabidopsis guard cell CO_2/HCO_3- response mutant screening by an aequorin-based calcium imaging system. *Plant Methods* 16, 59. doi:10.1186/s13007-020-00600-w

Wang, F., Gao, J., Yong, J. W. H., Liu, Y., Cao, D., and He, X. (2020). Glutamate over-accumulation may serve as an endogenous indicator of tricarboxylic acid (TCA) cycle suppression under NH_4^+ nutrition in wheat (*Triticum aestivum* L.) seedlings. *Environ. Exp. Bot.* 177, 104130. doi:10.1016/j.envexpbot.2020.104130

Wang, H., Hu, L., Xu, B., Chen, H., Cai, F., Yang, N., et al. (2020). Endoplasmic reticulum-targeted fluorogenic probe based on pyrimidine derivative for visualizing exogenous/endogenous H_2S in living cells. *Dyes Pigm.* 179, 108390. doi:10.1016/j.dyepig.2020.108390

Wang, R., Gu, X., Li, Q., Gao, J., Shi, B., Xu, G., et al. (2020). Aggregation enhanced responsiveness of rationally designed probes to hydrogen sulfide for targeted cancer imaging. *J. Am. Chem. Soc.* 142, 15084–15090. doi:10.1021/jacs.0c06533

Wegner, L. H., and Zimmermann, U. (2004). Bicarbonate-induced alkalinization of the xylem sap in intact maize seedlings as measured *in situ* with a novel xylem pH probe. *Plant Physiol.* 136, 3469–3477. doi:10.1104/pp.104.043844

Xu, J., Wang, Z., Zhang, M., Huang, C., Song, Y., Xu, F., et al. (2020). SQR mediates therapeutic effects of H_2S by targeting mitochondrial electron transport to induce mitochondrial uncoupling. *Sci. Adv.* 6, eaaz5752. doi:10.1126/sciadv.aaz5752

Zhao, N., Ding, B., Zhang, Y., Klockow, J. L., Lau, K., Chin, F. T., et al. (2020). Reactive oxygen species and enzyme dual-responsive biocompatible drug delivery system for targeted tumor therapy. *J. Control. Release* 324, 330–340. doi:10.1016/j.jconrel.2020.05.031

Zheng, Z., Zhou, T., Hu, R., Huang, M., Ao, X., Chu, J., et al. (2020). A specific aggregation-induced emission-conjugated polymer enables visual monitoring of osteogenic differentiation. *Bioact Mater.* 5, 1018–1025. doi:10.1016/j.bioactmat.2020.06.020

Zhong, K., Chen, L., Yan, X., Tang, Y., Hou, S., Li, X., et al. (2020). Dual-functional multi-application probe: rapid detection of H_2S and colorimetric recognition of HSO_3^- in food and cell. *Dyes Pigm.* 182, 108656. doi:10.1016/j.dyepig.2020.108656

Zhou, L., Cheng, Z.-Q., Li, N., Ge, Y.-X., Xie, H.-X., Zhu, K., et al. (2020). A highly sensitive endoplasmic reticulum-targeting fluorescent probe for the imaging of endogenous H_2S in live cells. *Spectrochimica Acta A-Molecular Biomol. Spectrosc.* 240, 118578. doi:10.1016/j.saa.2020.118578

Conflict of Interest: The authors declare that the research was conducted in the absence of any commercial or financial relationships that could be construed as a potential conflict of interest.